CHAPTER 2

LITERATURE REVIEW

2.1 Introduction

This chapter presents a review of relevant literatures on reflector-less Total Station and its application on deformation monitoring studies for determining and analyzing different kind of engineering structures, much of which has been published internationally. Special notes are made of those papers discussing the concepts and best practices of monitoring deformation, instrumentation, unstable slope along the highways, data collection, processing, representation and quality measure as well as related cases and issues pertaining to them. Other important sources such as textbooks and standards are also consulted and assessed.

2.2 Slope Failure in Malaysia

Numerous research projects on landslides or slope failure have been conducted in Malaysia over the last thirty years. Initially the investigations were carried out mostly to solve instability problems on site by geological investigation, which has been performed by the Geological Survey Department of Malaysia. The causes of landslides can be classified as external and internal causes. External causes are usually related to an increase of the shearing stress such as geometrical change, unloading the slope toe, loading the slope crest, shocks and vibration and change in water regime. While the internal causes are steeping of the slope, water content of the stratum and mineralogical composition and structural features, which tend to reduce the shearing strength of the

rocks [4]. Other causes of landslides include earthquakes and loud sounds. There have been 455 reported cases of landslides since 1961 and the dangers of more landslides occurring have been warned [5]. Most of the landslide prone areas are located at the hillsides.

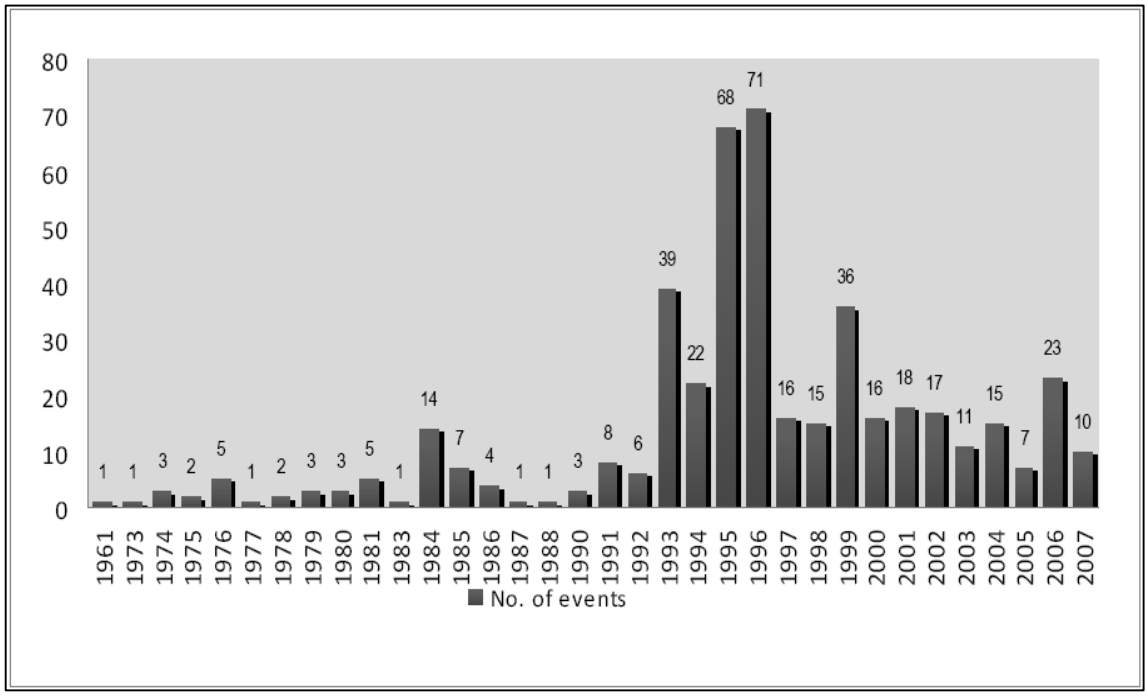

Figure 2.1 Number of Landslide Events in Malaysia (1961-2007)
(Source: G.S. Sew and W.S. Yun, 2008)

Based on 49 cases investigated [5], 60% of failure on man-made slopes are due to inadequacy in design alone. This design inadequacy is generally the result of a lack of understanding and appreciation of the subsoil conditions and geotechnical issues. In addition, failure due to construction errors alone either on workmanship, construction materials (poor quality, product failure and defects) and/or lack of site supervision contributed 8% to the total case of landslides. About 20% of the landslides investigated were caused by a combination of design and construction errors. Some catastrophic landslides that had occurred along the highway are listed in Table 2.1. In addition to those occurrences there are many new roads and highways that have the hazards of fatal slope failures. These include Ipoh – Changkat Jering Highway, East West Highway, Gerik, Perak, older road from Tapah, Perak to Cameron Highland, Kg. Raja to Pos Slim, Perak and Pos Slim to Loging Gua Musang, Kelantan.

Table 2.1 Number of Catastrophic Landslides in Malaysian

Date	Events	Locations
30 June 1995	20 people were killed in the landslide	Genting Highlands slip road near Karak Highway.
6 January 1996	A landslide occurred after a concrete wall collapsed, one person was killed	North-South Expressway (NSE) near Gua Tempurung, Perak.
December 2003	A rockfall at the interchange that caused the expressway to be closed for more than six months	New Klang Valley Expressway (NKVE) near Bukit Lanjan
31 May 2006	Four persons were killed in the landslides	Kampung Pasir, Ulu Klang, Selangor
26 December 2007	Two villagers were buried alive in a major landslide, which destroyed nine wooden houses.	Lorong 1, Kampung Baru Cina, Kapit, Sarawak.
17 January 2008	Two foreign workers were killed.	Cameron Highland.
17 October 2008	Two Indonesians were killed after they were buried alive by tones of sand in a landslide.	Ganesan Quarry, Hulu Langat near Kajang, Selangor.
19 October 2008	Four families evacuated from houses along the banks.	Sungai Kayu Ara in Petaling Jaya, Selangor.
22 October 2008	Tones of earth came crashing down a hill onto the grounds.	Taman Terubong Jaya apartments in Butterworth.
30 November 2008	Two sisters were buried alive when a landslide hit their bungalow.	Ulu Yam Perdana near Kuala Kubu Baru, Selangor.
6 December 2008	4 dead and 15 people injured in a major landslide.	Bukit Antarabangsa, Ulu Kelang, Selangor.

(Source: G.S. Sew and W.S. Yun, 2008)

Some case studies have reported landslides activities on various projects involving mining and ex-mining land, highways, hill side development and river bank instability studies at various parts of Malaysia. Most of the cases had occurred at hillside development in the urban areas and new highways such as at Cameron Highland. These can be referred to Figure 2.2 below.

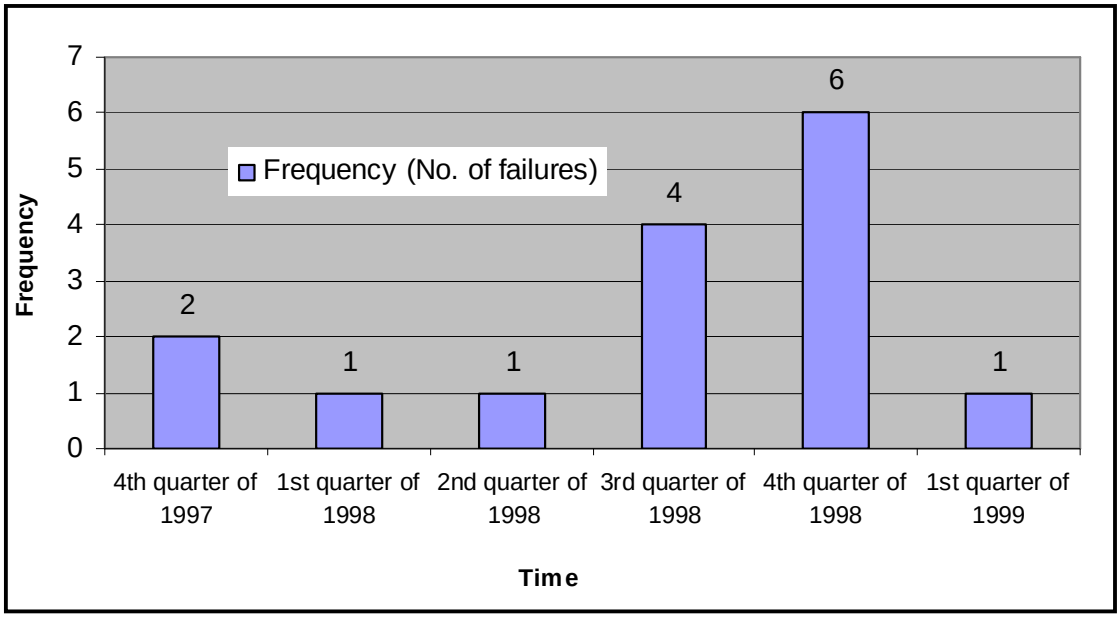

Figure 2.2 Frequencies of Slope Failures at Cameron Highland (Source: H. Omar, M. Daud, M. Zohadie, S. Maail, A. Azlan, and M. Ratnasamy, 2005)

From the graph it can be seen that most of the slope failures occurred at the end of the year, frequently in the third and fourth quarters due to heavy rainfall. The study on failure of cut slopes during construction of highways in mountainous areas, more failures occurred as the highway progressed into the highland regions and the instability problems of the cut slopes become more serious [6]. The rainfall data were used in analysis to determine the erosion risk frequency potential along the Cameron Highland – Gua Musang Highway, using rainfall data from 13 rainfall stations. They found that the relationship between rainfall and erosion risk is useful for erosion prevention [7].

Frequent occurrences of landslide in those areas during the rainy season have resulted in public fear for the safety of their lives and properties. This phenomenon has been accelerated by the rapid development especially at hilly terrain, construction of highways, mining activities, river bank instability, etc [8]. Therefore, activities such as land clearing, reclamation and rehabilitation should be implemented only after a thorough study on the impacts of soil erosion has been performed.

Most of the tragedies have been largely triggered by incidences of heavy rain either a single heavy rainstorm event or successive days of moderate rain during the rainy season. The real time rainfall values in the hilly terrain could serve as a useful indicator of the risk level of landslides. Therefore, monitoring the landslides and solving their mechanisms are very important to prevent and to reduce their negative effects [9].

2.3 About the Study Area

The road works are being carried out by MTD Construction Sdn. Bhd. under the Pos Slim to Ladang Blue Valley contract, a 35km section of Simpang Pulai – Lojing Highway project. The active landslide is located in the vicinity of CH 23+800. The road project was commenced in 1997 and landslides had occurred at roadside cuts at the site in the early years of the project. In September 2003, a large landslide took place on a hillside cutting at this prone area and it is still active. In 2006 the landslides moved as much as 2m. The active landslide is about 190m high and between 200m and 430m wide and its volume is estimated to be 2 to 3million m^3 as shown in Figure 2.3. The unstable slopes were cut back to flatter angles in an attempt to stabilize the ground but instability persisted [10], as shown in sequences in Figure 2.4. Eventually massive slope cutting-back works were undertaken but these still fail to create a stable hillside.

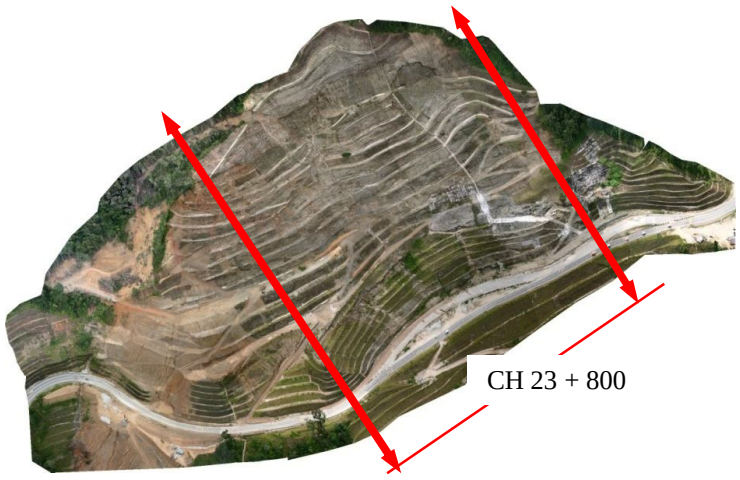

Figure 2.3 Overview of study area location, captured by aerial photograph
(Source: M. Ismail, 2008)

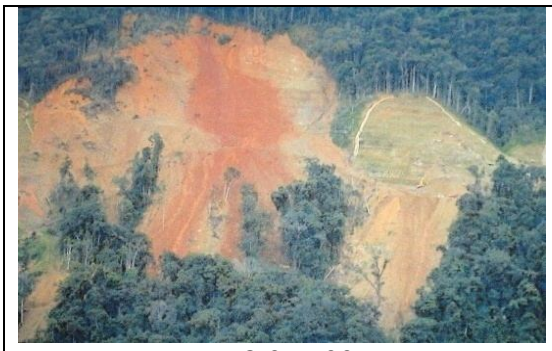

19.01.2001

20.10.2001

20.12.2001

05.01.2002

25.02.2002

14.02.2003

30.06.2003

23.12.2003

Figure 2.4 Sequences of land slide 2001 - 2003 at CH 23+800
(Source: M. Ismail, 2008)

2.4 Monitoring of Slope Failures

Land displacement monitoring in a certain landslide prone area in principle is the monitoring of changes in distances, height differences, angles and/or relative coordinates of the points (monuments) covering the area being studied. In this case, there are many methods and techniques that have been used for measuring landslide displacements. The examples are given in Table 2.2, which has been adopted and updated. Each of the monitoring method provides certain information on the state of landslides body. The table shows that each method has its own result, coverage and achievable accuracy level.

Table 2.2 Overview of methods used in measuring surface displacement and their precision

Method	Displacement Parameters	Typical Measurement range	Typical precision
Precision tape	Δ distance	< 30 m	0.5 mm / 30 m
Fixed wire extensometer	Δ distance	< 10 –80 m	0.3 mm / 30 m
Crack Meter	Δ distance	< 5 m	0.5 mm
Surveying triangulation	Δ X, ΔY, ΔZ	< 300 – 1000m	5 – 10 mm
Offsets from baseline	Δ H, ΔV	< 100 m	0.5 – 3 mm
Surveying traverses	Δ X, ΔY, ΔZ	Variable	5 – 10 mm
Geotechnical leveling	ΔH	Variable	2 – 5 mm/km
Precise Geotechnical leveling	ΔH	Variable	0.2 – 1 mm/km
EDM/Total Station	Δ distance	Variable (1 – 4 km)	1-5 mm + 1-5 ppm
Terrestrial photogrammetry	Δ X, ΔY, ΔZ	Ideally < 100m	20 mm - 100 m
Aerial photogrammetry	ΔX, ΔY, ΔZ	Hflight < 500m	100 mm
Inclinometer	Δ elevation angle	+/- 10º	5-10 mm + 1-2 ppm
GPS	ΔX, ΔY, ΔZ	Variable (usual < 20km)	2-5 mm + 1-2 ppm

(Source: J. A Gili, J. Corominas and J. Rius, 2000)

2.5 Deformation Survey

Deformation monitoring is a land survey activity during which repeated observations are made within a specified time frame for the purpose of detecting and quantifying movements of natural and man-made structures. The accuracies required in deformation survey depend on many factors, but generally it requires precise measurements with millimeter accuracy or better. In order to acquire the best survey technique that can be used throughout the deformation survey, elements of the systematic and random errors propagated in the observations must be taken into account. These are to make sure that the error values are less than the smallest displacement being measured or as expected [11]. A number of others factors are type and size of the structure, factors causing the movements (environmental) and whether an understanding of the movement is needed. The survey methods can be further subdivided into survey network method (geodetic method) and direct measurement method. In geodetic method, there are two types of geodetic networks namely the reference (absolute) and relative network [12], as shown in Figure 2.5.

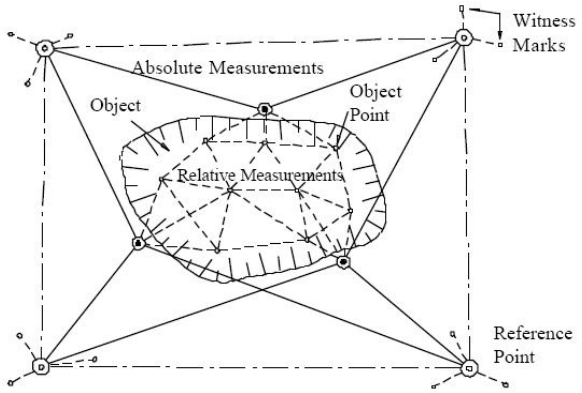

Figure 2.5 Object points representing the object under investigation are connected by geodetic measurements
(Source: M. Haberler and Weber, 2005)

The measurement of relative movement is generally much easier since movements are related to the object which monitor itself or to some arbitrary points which are located nearby. In these types of deformation, the points may move during a survey but the movements may not affect the results obtained. Meanwhile, for absolute measurements, most of the common points are related to datum points that are assumed stable during a monitoring survey.

2.6 Method of Deformation Analysis

Nowadays, the analysis of deformation survey is giving many contributions and is becoming more global to the industry in surveying, engineering, and geosciences. These matters have been discussed at many conferences often held especially by International Federation of Surveyors (FIG). The latest background and status of FIG activities on survey analysis deformation may be derived from the report given in 11th FIG symposium on deformation measurements [13]. Deformation analysis can be classified into two types; by using geometrical method and physical interpretation method. In geometrical methods, there are two types of trend analysis of the displacement all the common points in two epochs of observation. It consists of direct coordinates displacement, known as non-rigorous method, and robust and congruency testing method, also known as rigorous method [14]. In this research the direct coordinate's displacement were used in order to detect the deformation of the slope study.

2.7 Concepts and Procedures of Deformation Detection

Deformation detection is one of the most important measures in deformation monitoring. This is because all the way through deformation detection, the researcher can actually find out the displacement model or deformation movement (trend) for all the points in the monitoring network. Based on this information, the research object can be evaluated whether it is still in safe condition or otherwise. The main purpose of deformation detection is to ensure the stability of datum points, to monitor and determine deformation with reference to stable datum points and to prepare graphic presentation of deformation vector [15]. In observations, a special emphasis should be given to detecting and eliminating the gross errors. The characteristic point displacements are identified on the basis of at least two epochs and exclusively on identical network points. Geodetic technique like deformation analysis is able to handle stochastic data; geodetic deformation analysis is applied in e.g. terrestrial survey data. A statistical test is required to confirm the deformation detection results [16].

2.8 Types of Instruments and Techniques for Monitoring Deformation

There are many types of sensor that can be used for slope deformation monitoring. The selection of most appropriate technique or combination of techniques for any particular application will depend on cost, survey specifications and procedures, the accuracies required, and the scale of the survey involves. Therefore several aspects related to the optimal design of the networks, measurement and analysis techniques suited to the monitoring surveys have to be considered. As described by US Army Corps of Engineers (USACE).

Table 2.3 Accuracy Requirements for Structure Target Point (95% RMS)

Concrete Structures Dams, Outlet Works, Locks, Intake Structures	
Long-Term Movement Relative Short-Term Deflections Crack/Joint movements Monolith Alignment Vertical Stability/Settlement	± 5 - 10 mm ± 0.2 mm ± 2 mm
Embankment Structures Earth-Rock fill Dams, leaves	
Slope/crest Stability Crest Alignment Settlement measurements	± 20 – 30 mm ± 20 – 30 mm ± 10 mm
Control Structures Spillways, Stilling Basins, Approach/Outlet Channels, Reservoirs	
Scour/Erosion/Silting	± 60 -150 mm

(Source: S. Joseph, 2002)

2.8.1 Monitoring by Instrumentation Techniques

Geotechnical and structural methods are usually adopted by civil engineers using special equipments as shown in Figure 2.6. This is to measure the changes in length (extensometer), lateral earth movements (inclinometer) and etc. These instruments are widely used and may be installed on the slope surface. The settlement gauge is a device to measure the horizontal or vertical displacements at points parallel to the surface and is normally used to measure movement at several locations within rock fill embankments [17]. While strain meter, was widely used in boreholes to measure small changes in the diameter of the borehole. Other instrument used is the crack meter; this tool is very useful in the early detection of deforming mass movements and it measures between two points on the surface, which have signs of separation. The inclinometer is very useful for measuring a tilt or angle of slope and piezometer is a tool for measuring the pore pressure of the groundwater or water pressure within a geological structure [18].

Figure 2.6 Geotechnical Methods and Special Instruments
(Source: C.D. Hill, and K.D Sippel M, 2002)

All the instruments mentioned above are known as instrumentation techniques and those methods could give descriptions in the local system only compared to geodetic methods which can give a more global deformation description [19]. The combination of the above instruments (Figure 2.6) can also be used as a slope indicator. The tool manufactures a full range of geotechnical and structural sensors for monitoring tilt, displacement, pressure, and strain at the same time.

Generally those methods mentioned above are able to measure the slope deformation accurately (until sub-millimeters level of accuracy). However, the geotechnical methods give limited information of the subsurface of the deformable body, which is capable of providing measurement in one dimension [20]. This technique requires the instruments to be fitted on the deformable body such as open mining slopes or steep slopes, which means if the slope collapses, the instruments will be carried together with the mass. The combination of inclinometer or strain meter instrument and Global Positioning System (GPS) or Total Station is suitable and can produce good results in dam deformation monitoring [21]. Details about those methods will not be discussed in this thesis.

2.8.2 Monitoring by Observational Techniques

On the other hand, in geodetic method which is highly understood by land surveyors, special measuring techniques can be applied such as Global Positioning System (GPS), close range photogrammetry, remote sensing, Very Long Baseline Interferometry (VLBI), Satellite Laser Ranging (SLR), Total Station and precise leveling (terrestrial survey). These techniques mostly used observational techniques and more quantitative than geotechnical techniques. The main techniques, terrestrial survey with reflector-less Total Station generally used are discussed in the following sections.

2.8.2.1 Global Positioning System (GPS)

With the development of Global Positioning System (GPS) and computer science, the GPS of navigation satellites now can be used for the real-time deformation monitoring of

slope failure or others large structures. With the sampling frequency of Global Positioning System (GPS) receiver can reach about 20 times per second, while the location precision can approach 2 - 5 mm ± 1-2 ppm (parts per million). Global Positioning System (GPS) can provide a solution to these problems by providing a continuous or quasi-continuous 3 Dimension time-series data, while also maintaining a high level of precision and operating with minimal user intervention. There were several methods in GPS observation, such as Static methods, Fast Static and Real Time Kinematics (RTK-GPS). All the methods mention above depend on the application and the needs. Usually the static methods are useful for high precision and for long terms deformation monitoring. The observation period for the first epoch and the epoch second necessary at least three months or over, in order to get better results.

While Fast Static (FS-GPS) and Real Time Kinematics (RTK-GPS) methods applied for deformation of small areas. Apart from accuracy factor that can reach up to 5mm ± 1ppm [22], Rapid Static techniques are accepted as GPS data collection's method because its applicable procedures on location which possess obstacle problem satellite such as tree leaves and hilly area [23]. Although GPS provides a valuable tool for monitoring, some environments are not ideal for GPS [24].

2.8.2.2 Remote Sensing Method

Remote sensing is a technology to sense phenomena without contact; it includes two branches of photogrammetry and remote sensing. In photogrammetry, 3-D surfaces are reconstructed from a pair of so-called stereo images, which were taken of the same object but from two slightly different angles. It makes use of the optical geometry of two images. On the other hand, in remote sensing, a number of sensors are used to take images. Each sensor records the energy of electromagnetic waves of limited wavelength (or frequency). The waves would be radiated from or reflected by phenomena. Remote sensing makes use of the reflectance of different waves by phenomena.

Recently, terrestrial laser scanning systems become a new technology tools in slope monitoring. It can easily acquire large amounts of point cloud in a short time and offer high density and accurate information. It collects data in complex condition, scans a series of large, complicated and irregular expanse quickly, so it can get 3D datum and analyze the status of landslide area by software. The ground-based 3D laser scanner is a technique of non-contact and active remote sensing. This system can provide the colorful images and deploy by a single operator. The work efficiency is high and the surveyor does not need to arrive at the dangerous region to set up the GPS stations or the prism spots [25]. Unfortunately, this system is still new in our country and expensive.

2.8.2.3 Terrestrial Survey Method

These methods are also known as ground based geodetic technique. Currently they are a quite a number of new technology in measuring the distance, angles and height. These parameters are crucial in deformation monitoring of large structure, landslides or slope failure along the highways. Continuous data recording from instrument like Total Station, using established baseline, can be used for monitoring the health of engineering structures, and thereby be useful for the public safety of civil, structural and earthquake engineering [26]. Total Station instruments have replaced theodolites and tachymeter and can accomplish not only all angle measurements but also accurate and quick distance measurements. Furthermore, they can make computations with angle and distance measurements and display on a liquid crystal display (LCD) in real time. With the aid of trigonometry, the angles and distances may be used to calculate the actual positions (northing, easting and elevation) of surveyed points in absolute terms. In addition, to provide guidance to user, the instrument comes together with microprocessors to perform many different types of computations. These include averaging of multiple angle and distance measurements, correcting electronically measured distances for prism constants, atmospheric pressure and temperature and etc.

2.9 New Generation of Total Station (TS) Instruments

Recently, survey equipment manufacturer has developed their new technology based on research and development for the new survey equipments such as Total Station. To satisfy this ever-growing demand, solutions are needed which not only meet, but exceed user requirements. The latest type of the TS instruments is the reflector-less TS, robotic TS, and imaging TS. Imaging TS allow users to capture digital field images and combine images to create high-accuracy 3D models. TS with integrated GPS tool can be used as a standalone system, while a Smart Antenna can be used as a Real Time Kinematic (RTK) rover on a pole, and the total station can be used alone with full functionality as a conventional or robotic instrument. This outstanding instrument sets new standards in scalability, accuracy, productivity and ultimately, in productivity.

Over the last two decades, electronic TS devices have largely used in monitoring of landslide. A new technology of TS instrument can be used effectively to monitor slope stability. A near real-time monitoring system currently been used as a warning systems as shown in Figure 2.7. The monitoring system, such as ALERT [27] can provide fully automated data collection and analysis the displacements within a second.

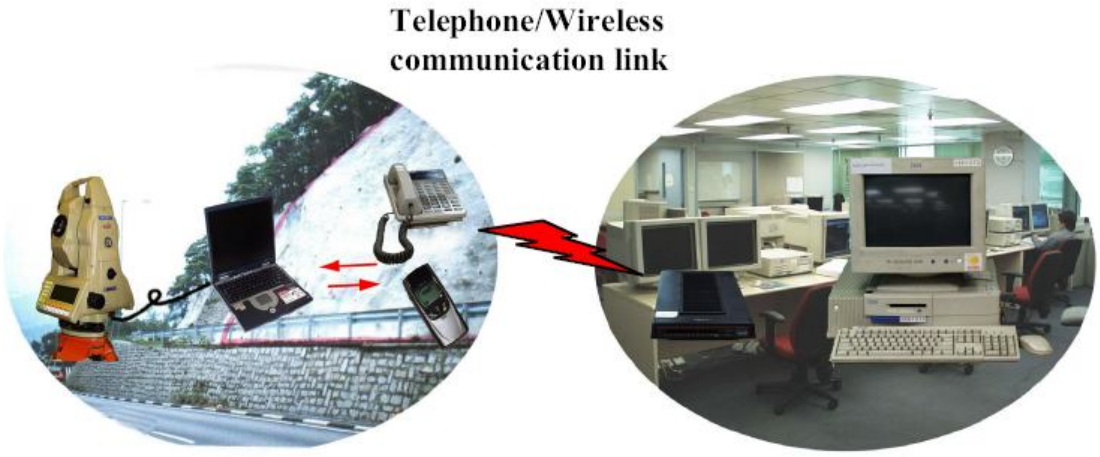

Figure 2.7 Real Time Monitoring System.
(Source: A. Chrzanowski, G. Bastin and R. Wilkins, 2003)

The concepts of measurement by TS survey method is by observing the monitored points (prisms) which have been planted as a permanents points on the slope area. An angles (bearing) and distance or intersection method have been used on as the observables. Each observed points can provide 3D coordinates which were used to determine the displacements or the magnitude of the deformation. However with new TS technology, such as reflector-less TS, the prisms can be replaced with any identical target as monitoring points. In order to achieve good results in observation, the observation data should be free from some sources of random errors which will in fact the quality of the measured data. The major error sources include instrument placement and leveling, target placement, circle reading, and target pointing. The effects of reading, pointing, and leveling errors can be reduced by increasing the number of the observations and the effects of instrument and target setup errors can be reduced by increasing sight of distances as suggested by Wolf and Ghilani [28].

Alongside the Total Station measurement, there is another conventional terrestrial surveying technique that can be used to monitor a land deformation. It is a precise leveling technique. This technique is able to provide only one dimension information (elevation or difference height), it is the most precise method of monitoring local vertical deformations. This technique can provide a vertical component precision of 0.2 to 1 parts per million (ppm) of the level run length [29]. Although accurate, this technique is relatively slow and time consuming in its execution, especially when precise leveling procedures are being implemented. Disadvantages of the technique are the surveys crews must be go across directly on the unstable surface, and it must also be initiated from a stable monument situated outside the zone of deformation. Due to the ineffectiveness, recently this method is not favored [30].

2.10 Types of Reflector-less Total Station

Starting with the LEICA DIOR3002 in 1986, reflector-less Total Station technologies develop very stupendously. Whereas Disto laser distance meter have replaced the common measuring tape almost completely, up to date Total Station can allow the users switching from Total Station with a reflector to a mode without reflector to measure the data. This technology is very practical in deformation monitoring on dangerous and inaccessible areas. Items of economic, advantage of reflector-less Total Station increase with the number of surveyed points and do no longer have to be fitted with prisms.

There are two types measuring methods, based on the Phase Shift method and based on patented Pulsed Laser Time-of Flight methods. Phase Shift method is designed to measure extremely accurate short-range distances to cooperative and non-cooperative targets, as given on Figure 2.8. While Pulsed Laser Time-of Flight methods provides the longest range, as shown on Figure 2.9. A time of flight systems measures range, ρ, by observing the two way travel times, Δt, of pulse of laser light [31]. These types of Total Station was used and applied in this research for deformation monitoring slope failure because it can provide long distance measurement. However, the accuracy of the measurement to various material targets is still doubtful, because each material have different reflecting surface, therefore calibration for this instrument is necessary to be accomplished before data collection is performed.

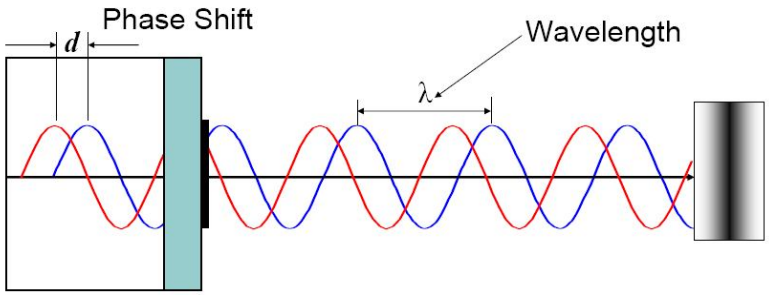

Figure 2.8 Phase Shift EDM (Distance = ½ (m x λ + d)
(Source: M. Ted and W. Brain, 2007)

Where,

m	-	Number of full wavelengths
λ	-	Modulation wave length
d	-	Phase Shift

Figure 2.9 Timed Pulse EDM
(Range = Time x Speed of light /2 = ½ c. Δt)
(Source: M. Ted and W. Brain, 2007)

Where,

Δt	-	Two way travel times
c	-	Speed of light

2.11 Theory of Errors Propagation in Total Station Observations

In composing the errors budget of the observation, consideration of the contribution of all random errors sources must be knowledge. These include internal sources (e.g., noise in the observations, beam width uncertainty) and external sources (e.g., the survey points used and instrument setup errors). Therefore all quantities that are measured directly contain errors and any value computed from them will also have errors. Total Station observation can provided 3D data, which means sources of errors before the final coordinates computed would come from angle, the distance and elevation. These sources of errors must be used to determine the estimated errors in functions that use these computed values, such as determination of latitudes and departures.

2.11.1 Error Propagations in Distance Observation

As a general concept in measurement, no measurement is perfect, hence every measurement contains error; true value of a measurement is never known; and the exact size of the errors present are always unknown [32]. Thus the distances measured by using a Total Station is also not free from errors. Commonly a calibration process is required to ensure that the Total Station has a certain acceptable error threshold, which

provides evidence that the equipment is in good conditions and is capable of providing reliable data. The error affecting Total Station measurement can be divided into internal and external components. Internal errors include zero, scale, cyclic, and phase measurement errors. While, external errors are mainly due to atmospheric refraction. All distances measured by the Total Station and reflector combination have a constant error, which is generally caused by three main factors:

i. Electrical delays, geometric detours, and eccentricities in the Total Station;
ii. Differences between the electronic centre and the mechanical centre of the Total Station;
iii. Differences between the optical and mechanical centre of the reflector.

Additional constant correction is needed to correct the measured distances from those differences [33]. These can be referred to Figure 2.10 where it is the basic of principles of electronic distance measurement (EDM). The addition constant **a** applies to a Total Station consisting of distance meter and reflector. The components **e** and **r** are auxiliary quantities.

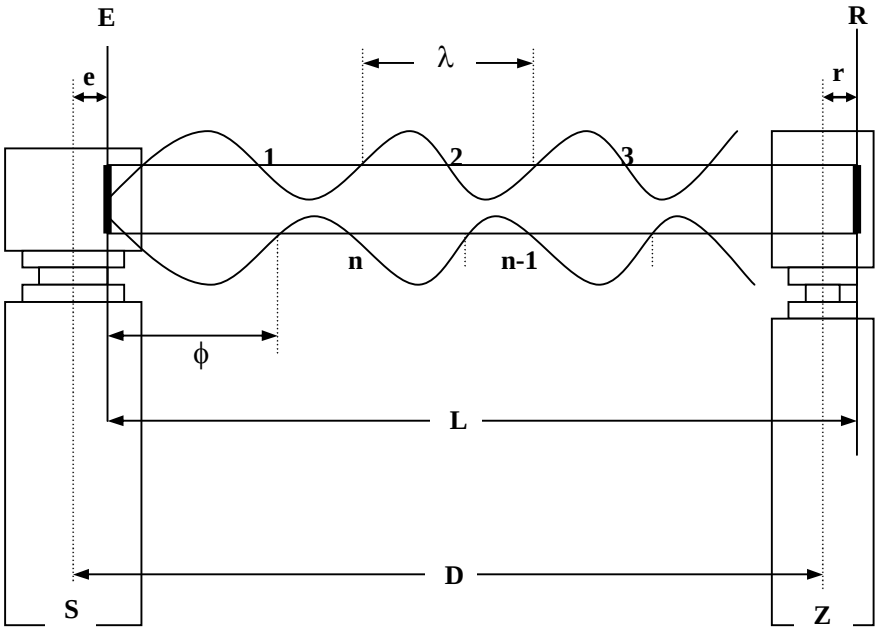

Figure 2.10 Principles of Electronic Distance Measurement (EDM)

Where,

S	-	Station
Z	-	Target
E	-	Reference plane within the distance meter for phase comparison between transmitted and received wave
R	-	Reference plane for the reflection of the wave transmitted by the distance meter
a	-	Addition constant
e	-	Distance meter component of addition constant
r	-	Reflector component of addition constant
λ	-	Modulation wave length
ϕ	-	Fraction to be measured of a whole wave length of modulation ($\Delta\lambda$)

Scale error is an incremental systematic error which is linearly proportional to the length of measured distances. It can arise from variations in the modulation frequency of the Total Station, non-homogeneous emission/reception patterns from the emitting/receiving diodes (in-homogeneities of phases), un-modeled variations in atmospheric conditions and errors in the collection and use of atmospheric data [34]. Cyclic error is a periodic systematic error. Cyclic error is a function of internal phase measurement of Total Station. Phase measurement error is caused by unwanted feed through the transmitted signal onto the received signal [34]. Cyclic error normally is sinusoidal with a wavelength equal to the unit length of the Total Station. Unit length is equal to one half of the modulation wavelength of TS [35]. As cyclic error repeats itself for every unit length contained within a measured distance, its sign and magnitude depend on the length of measurement. Magnitude of the cyclic error usually increases parallel with age of the Total Station.

Calibration of the Total Station is usually carried out using baselines and techniques involving both unknown and known baseline lengths [35]. The simplest method to determine the zero error of the Total Station is called three peg tests; it involves three

unknown points, as shown in Figure 2.11. During the calibration, all three distances are measured and $l_{12,}$ l_{23} and l_{13} are obtained.

$$l_{12} = d_1 + z$$
$$l_{23} = d_2 + z$$
$$l_{13} = d_1 + d_2 + z$$

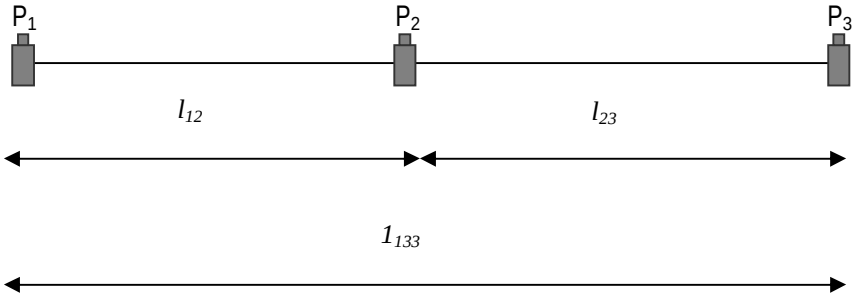

Figure 2.11 Three Peg Tests
(Source: Landgate, 2008)

Where, d_1 and d_2 are the correct distances from 1 to 2 and from 2 to 3. Which means zero error is given as $z = l_{13} - (l_{12} + l_{23})$. However to determine scale error, standard baseline such as those which can be obtained from the relevant government departments (JUPEM) or geodetic test line must be used, as shown in Figure 2.12 [36]. Whereas, the constant and scale factor are determined by measuring all combinations of the distances. Least squares adjustment formula is used to determine the constant and scale factor.

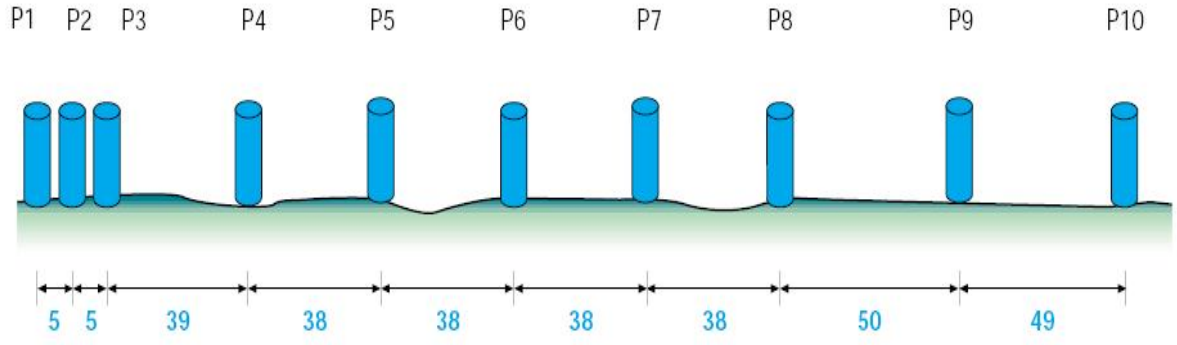

Figure 2.12 Standard Pillars for EDM Baseline
(Source: JUPEM, 2002)

The variance of the distance model can be expressed as in the following formula [40];

$$\sigma_D^2 = a^2 + (D \times b\ ppm) \qquad \text{Eq.2.1}$$

Where,

σ_D^2 = Variance of total distance

a (mm) and b (part per million) = Instruments specified accuracy parameters

D = Distance (km)

2.11.1.1 Constant Error for Different Reflecting Surface Materials

Reflector-less TS was made for measuring distance measurements without cooperative targets or prism. A different reflecting surface material produces different constant error result. Therefore a test was done to make fair comparison of range performance and accuracy of the variable materials. According to Trimble, Kodak Neutral Test card as shown in Figure 2.13, commonly called the Kodak gray card and Kodak white standard card were used as an appropriate standard card in comparing constant error in direct reflex EDM technology instruments [37]. This paper is recognized as a standard material in professional photography. The gray side, known as Kodak Gray, reflects precisely 18% of the white light that strikes it, meanwhile the Kodak White, reflects precisely 90%.

Figure 2.13 The Kodak Neutral Test Card
(Source: R. Hoglund and P. Large, 2002)

Based on the field test, Kodak Gray Card produces less accuracy than Kodak White Card. This is due to reflecting factor where light condition and the surface reflectance at the target influence the range. This can be seen in Figure 2.14 as tested by Trimble Direct Reflect (DR) Total Station Instruments.

Surface	DR300+	DR Standard
Kodak 90%	>800 m (2,625 ft)	>240 m (787 ft)
Kodak 18%	>300 m (984 ft)	>120 m (393 ft)
Concrete	>400 m (1,312 ft)	>100 m (328 ft)
Wood	>400 m (1,312 ft)	>200 m (656 ft)
Light Rock	>300 m (984 ft)	>150 m (492 ft)
Dark Rock	>200 m (656 ft)	>80 m (262 ft)

Figure 2.14 Direct Targets to Various Surfaces
(Source: R. Hoglund and P. Large, 2002)

In some case 28 studies, research has been carried out to determine the tolerance of measurement with various surfaces, mostly with different reflection characteristics such as colour, texture of materials and also the effect of angle of incidence in the measurements, example when measuring to corners of target point having different shapes. The selection of testing materials is based on materials that are often used in construction (concrete), architectural (various colours of walls, wooden surfaces, ceramic tiles and etc), industrial (porcelain), agricultural, forest and archeological sites [38]. Their results show that materials with uneven surface such as concrete block, rough black wood, brown mud surface and black coloured surfaces give larger constant errors than white smooth surfaces, examples such as white smooth ceramic tile, white porcelain tile or any white coloured materials. The initial results of the test performed by Ali were summarized in Figure 2.15 below [38]. The test was done using LEICA TCR 1102.

Reflector Type	Computed reflector/inst. Constant (mm)	Maximum distance measured (m)
Concrete block	11.2	40
Unpainted steel bracket	9.8	46
Rough black wooden	10.7	20
A brown mud surface	14.3	22
Smooth black wooden	13.1	60
A white zinc sheet	9.4	62
Rough white wooden	9.3	80
Smooth white wooden	9.1	80
White smooth porcelain tile	9.0	100
White smooth ceramic tile	6.9	95
Steel bracket painted white	7.1	77
Black smooth porcelain	9.7	70
Black smooth ceramic tile	9.8	72

Figure 2.15 Constant Errors of Various Reflecting Materials
(Source: S. Ali, 2008)

This outstanding instrument sets new standards in scalability, accuracy, productivity and ultimately, in productivity. Some of the documented applications of reflector-less TS in deformation monitoring include landslide monitoring [39], structural assessment of a bridge [40] and mapping of the interior of a monastery dome [41].

2.11.2 Error Propagations in Angle Observation

When observing an angle, the major error sources include instrument placement and leveling, target placement, circle reading and target pointing, as shown in Figure 2.16. There are three components in total station that can cause these errors, vertical axis, horizontal axis and axis of sighting, as shown in Figure 2.17. These errors normally occur after the instruments and the target prism have been setup on the ground during the observation. Each of these sources produces random errors. These errors may be small or large and it depends on the instrument, the observer, and the conditions at the time the angle measurement is made. With the introduction of electronic theodolites and later known as total station instruments, the standard deviation in angle measurements has a new standard called DIN 18723[42]. DIN stands for "Deutsches Institut für Normung", which means "German Institute for Standardization".

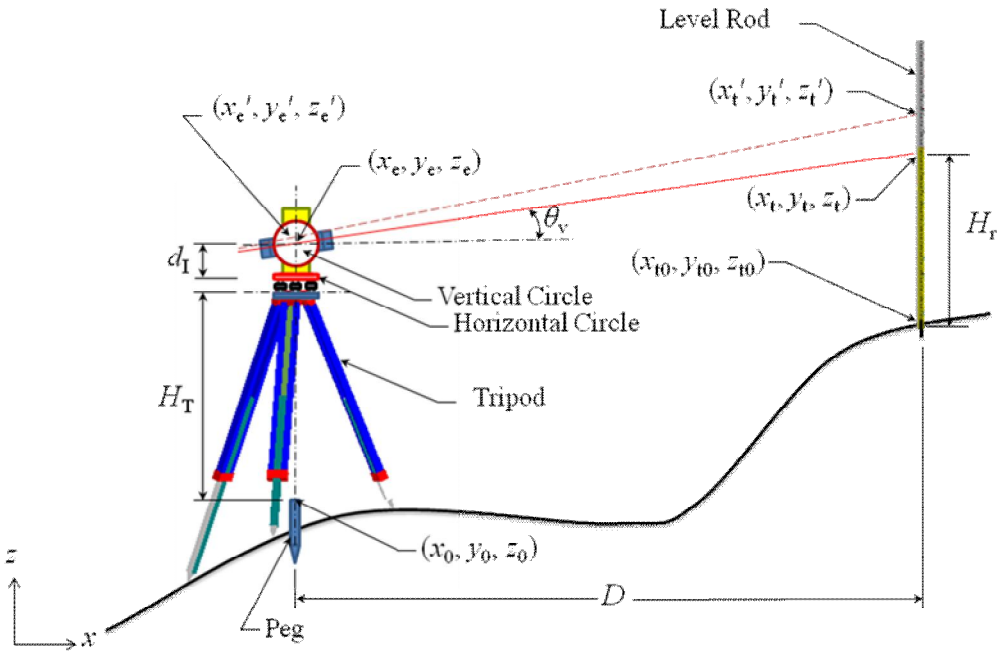

Figure 2.16 Simulation of Virtual Survey Scenario
(Source: S.S.Ruei, L.C.Cho, K.C.Shin and H.H.Shang, 2008)

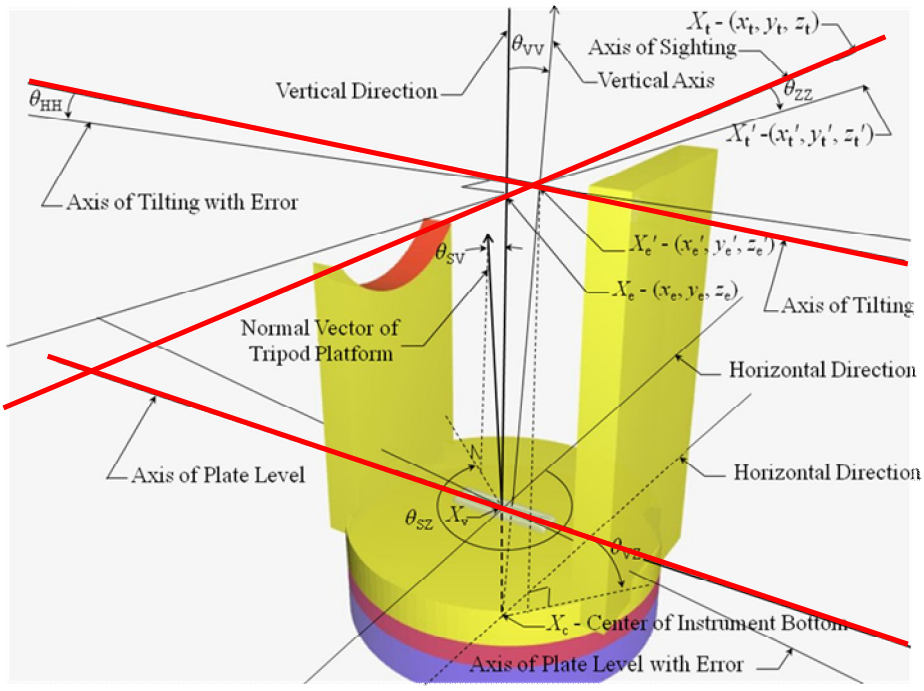

Figure 2.17 Reference Axes of Total Station
(Source: S.S.Ruei, L.C.Cho, K.C.Shin and H.H.Shang, 2008)

2.11.2.1 Pointing and Reading Errors with Total Stations

The value provided by the standard DIN 18723 is shown in detail in the specification of the Total Station instruments. Thus, in terms of a single pointing and reading error, σ_{pr} the DIN value, σ_{DIN} can be expressed according to the following formula [42].

$$\sigma_{DIN} - \frac{\sigma_{pr}\sqrt{2}}{2} - \frac{\sigma_{pr}}{\sqrt{2}} \qquad \text{Eq.2.2}$$

Using this equation, the expression for the estimated error in the observation of a single direction due to pointing and reading with electronic theodolite is as follows:

$$\sigma_{pr} = \sigma_{DIN}\sqrt{2} \qquad \text{Eq.2.3}$$

The estimated error in an angle measured for the *n* times and averaged due to pointing and reading is given below:

$$\sigma_{\alpha pr} = \frac{\sigma_{pr}\sqrt{2}}{\sqrt{n}} \qquad \text{Eq.2.4}$$

Substituting equation (2.3) into equation (2.4) yields the following equation:

$$\sigma_{\alpha pr} = \frac{2\sigma_{DIN}}{\sqrt{n}} \qquad \text{Eq.2.5}$$

2.11.2.2 Target Centering Errors

Effect of centering error refers to the inability to exactly align the center of the instrument and the target with the survey marker. The magnitude of centering error depends on the method and equipment used good weather conditions such as no wind and considering that the equipment is in good. The expected centering errors for different types of centering equipment under good weather and equipment conditions are as listed in Table 2.4 [43].

Table 2.4 Centering Errors for Different Types of Centering Equipments

Method of Centering	Expected Error
String plumb bob	1 mm/m
Optical plummet	0.5 mm/m
Plumbing rods	0.5 mm/m
Forced or self-centering	0.1 mm

(Source: S.L. Kuang, 1991)

An estimate of the effect of this error in angle observations can be made by analyzing its contribution to a single direction as shown in Figure 2.18. The angular error due to centering error depends on the position of the target. If the target is on line but off center, as shown in Figure 2.18(a), the target centering error does not contribute to the angular error. However, as the target moves to either side of the sight line, the error size increases. As shown in Figure 2.18(d), the largest error occurs when the target is offset perpendicular to the line of sight. The maximum error in an individual direction due to target centering error is given in the equation below:

$$e = \pm \frac{\sigma_d}{D} \text{rad} \qquad \text{Eq.2.6}$$

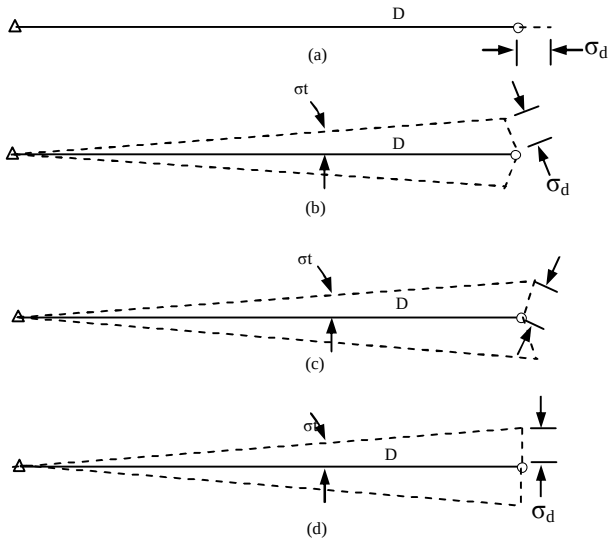

Figure 2.18 Possible Target Locations

Where *e* is the improbability in the direction due to the target centering error, σ_d the amount of centering error at the time of pointing, and as shown in Figure 2.19 *D* is the distance from the instrument center to the target. Two directions are required for each angle observation.

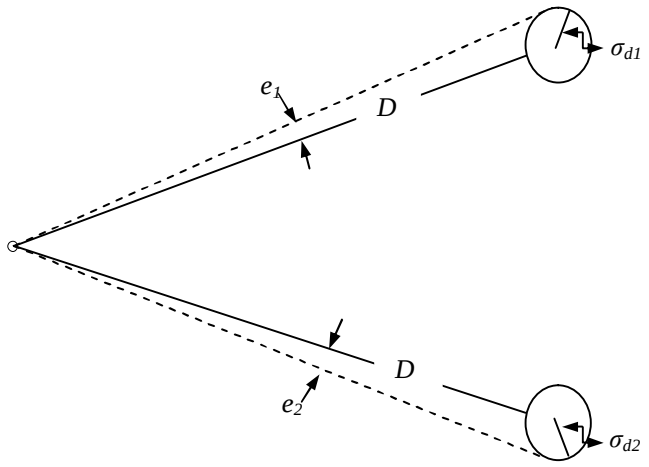

Figure 2.19 Errors in an Angle Due to Target Centering Error

The contribution of the target centering error to the total angular error is given below, the equation are unit less.

$$\sigma''_{\alpha t} = \sqrt{\left(\frac{\sigma_{d1}}{D_1}\right)^2 + \left(\frac{\sigma_{d2}}{D_2}\right)^2} \qquad \text{Eq.2.7}$$

Where, $\sigma_{\alpha t}$ is the angular error due to the target centering error, σ_{d1} and σ_{d2} are the target centering errors at station 1 and 2, respectively, and D_1 and D_2 are the distances from the target to the instrument at station reference object and monitoring target. Since the monitoring target point is a mini prism pole, a plumbing rod is used to determine the ability to center the target. The target centering errors at station 1 and 2 can be stated as $\sigma_{d1} = \sigma_{d1} = \sigma_t$. In order to convert the result to arc seconds, it must be multiplied by the constant ρ (206,264.8"/rad); hence Equation 2.8 below is yielded.

$$\sigma''_{\alpha t} = \sqrt{\frac{D_1^2 + D_2^2}{D_1 D_2}}\sigma_t(\rho) \qquad \text{Eq.2.8}$$

2.11.2.3 Instrument Centering Errors

This error depends on the quality of the instrument and the state of adjustment of its optical plummet, the quality of the tripod, and the skills of surveyor during instrument setup.

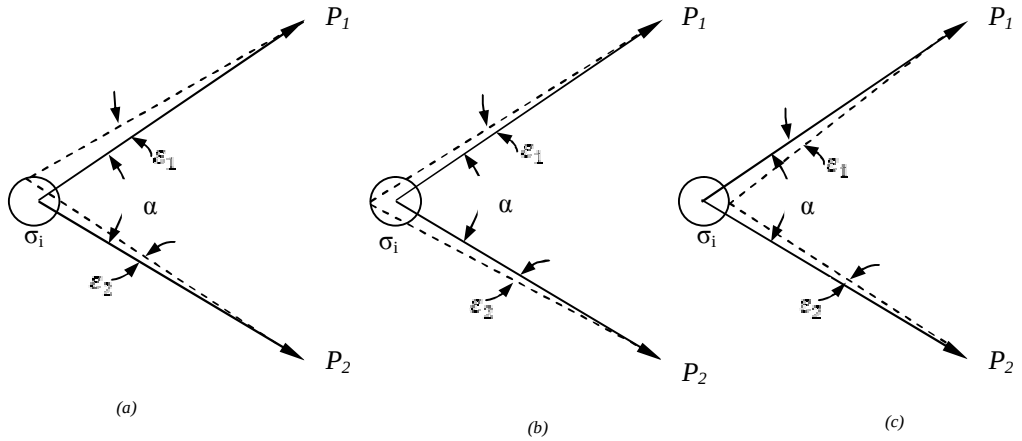

Figure 2.20 Errors in an Angle due in Instrument Centering

The error can be compensated, as shown in Figure 2.20(*a*), or it can be maximized when the instrument is on the angle bisector, as shown in Figures 2.20(*b*) and (*c*). For any individual setup, this error is a constant; however, since the instrument's location is random with respect to the true station location, it will appear to be random in the adjustment of network which involves many stations. From Figure 2.20, the true angle α is:

$$\alpha = (P_2 + \varepsilon_2) - (P_1 + \varepsilon_1) = (P_2 - P_1) + (\varepsilon_2 - \varepsilon_1) \qquad \text{Eq.2.9}$$

Where P_1 and P_2 are the true directions and ε_1 and ε_2 are errors in those directions due to faulty instrument centering. The error size for any setup is given by:

$$\varepsilon = \varepsilon_2 - \varepsilon_1 \qquad \text{Eq.2.10}$$

The error in the observed angle due to instrument centering errors is analyzed by propagating errors in a formula based on *(x, y)* coordinates. In Figure 2.21 a coordinate system has been constructed with the *x* axis going from the true station to the foresight

station. The *y* axis passes through the instrument vertical axis and is perpendicular to the *x* axis.

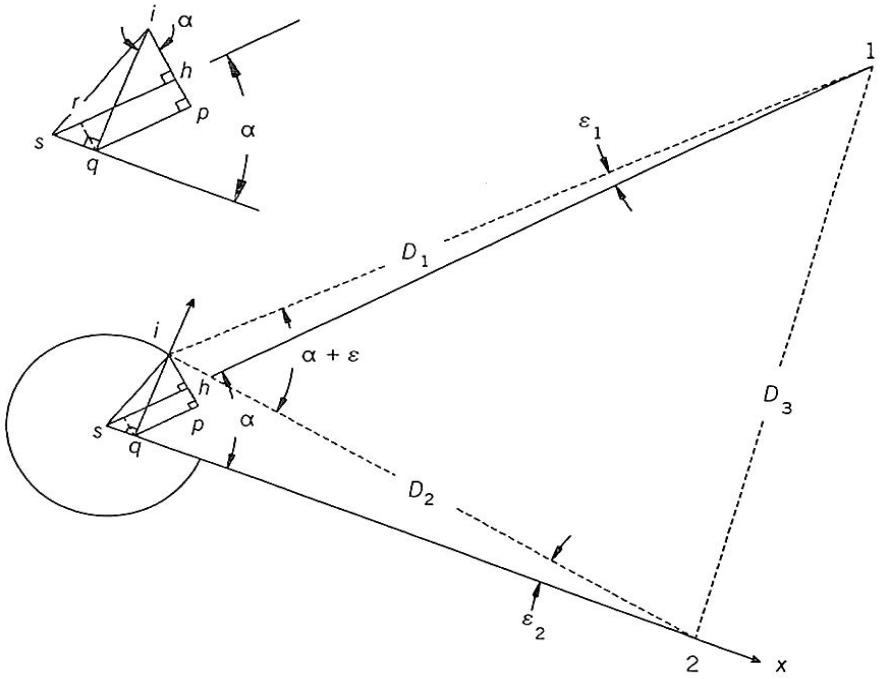

Figure 2.21 Analysis of Instrument Centering Error

From the above figure, the following equations can be derived:

$$ih = ip - qr$$

Eq.2.11

$$ih = iq\cos\alpha - sq\sin\alpha$$

Letting $sq = x$ and $iq = y$, Equation 2.11 can be rewritten as:

$$ih = y\cos\alpha - x\sin\alpha \qquad \text{Eq.2.12}$$

From Figure 2.21,

$$\varepsilon_1 = \frac{ih}{D_1} = \frac{y\cos\alpha - x\sin\alpha}{D_1} \qquad \text{Eq.2.13}$$

$$\varepsilon_2 = \frac{y}{D_2} \qquad \text{Eq.2.14}$$

By substituting Equations 2.13 and 2.14 into Equation 2.10, the error in an observed angle due to instrument centering error is given by the equation below:

$$\varepsilon = \frac{y}{D_2} - \frac{y\cos\alpha - x\sin\alpha}{D_1} \qquad \text{Eq.2.15}$$

Reorganizing Equation 2.15 yields

$$\varepsilon = \frac{D_1 y + D_2 x\sin\alpha - D_2 y\cos\alpha}{D_1 D_2} \qquad \text{Eq.2.16}$$

Taking partial derivative of Equation 2.16 with respect to both *x* and *y* gives

$$\frac{\partial\varepsilon}{\partial x} = \frac{D_2\sin\alpha}{D_1 D_2}$$

$$\frac{\partial\varepsilon}{\partial y} = \frac{D_1 - D_2\cos\alpha}{D_1 D_2} \qquad \text{Eq.2.17}$$

Therefore Equation 2.17 can be rewritten in algebraic form as

$$\sigma_\varepsilon^2 = \frac{D_2\sin\alpha}{D_1 D_2}\sigma_x^2 + \frac{D_1 - D_2\cos\alpha}{D_1 D_2}\sigma_y^2 \qquad \text{Eq.2.18}$$

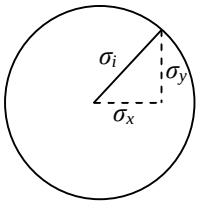

Figure 2.22 Instrument Centering Error at a Station

From Figure 2.22 assuming that estimated errors in the *x* and *y* axes are σ_x and σ_y. Then the errors is $\sigma_x = \sigma y - \frac{\sigma_i}{\sqrt{2}}$.

Letting $\sigma_\varepsilon = \sigma_{\alpha i}$, expanding the squares of Equation 2.18, and rearranging yields:

$$\sigma_{\alpha i} = \frac{D_1^2+D_2^2(\cos^2\alpha+\sin^2\alpha)-2D_1D_2\cos\alpha}{D_1^2D_2^2}\frac{\sigma_1^2}{2} \qquad \text{Eq.2.19}$$

By making the trigonometric substitutions of $\cos^2\alpha + \sin^2\alpha = 1$ and $D_1^2 = D_2^2 - 2D_1D_2\cos\alpha = D_3^2$ in Equation 2.19, taking the square root of both sides, and multiplying by ρ (206,264.8"/rad) to convert the results to arc second's yields:

$$\sigma''_{\alpha i} = \pm\frac{D_3}{D_1^2D_2^2}\frac{\sigma_1}{\sqrt{2}} \qquad \text{Eq.2.20}$$

Therefore the standard deviation of a sum of the estimated angular error by using total station is the combined error from Equations 2.5, 2.8 and 2.20, as expressed in Equation 2.21 below.

$$S_{dA} = \sqrt{\sigma''^2_{\alpha t} + \sigma''^2_{\alpha i} + \sigma''^2_{\alpha \rho}} \qquad \text{Eq.2.21}$$

2.11.3 Error Propagations in Elevation Observation

One of the advantages of using the reflector-less Total Station in measuring is the elimination of target heights or prism poles measurement, which no need someone to measure the targets height or prism poles at the inaccessible area. By using Total Station with a data recorder or by using program on board the horizontal direction, zenith angles and EDM (Electronic distance measurement) distances can be observed simultaneously. The basic concept to transfer trigonometrically leveled heights from the trunnion axis of the Total Station to each surveyed ground mark is the instrument and reflector heights must be measured accurately [44].These is described in Figure 2.23 below.

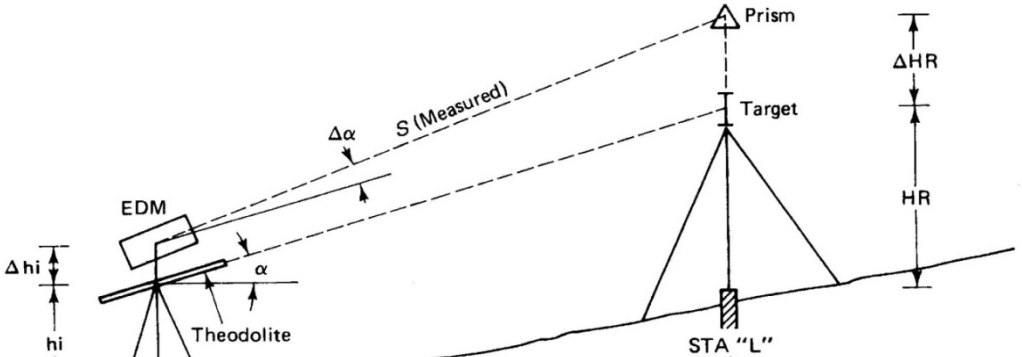

Figure 2.23 Determination of Elevation Difference by Trigonometric Leveling

Additional problem in determination of elevation is computation of correction to vertical angle ($\alpha\Delta$) that occurs when different instrument height (Δhi) and different reflector height (ΔHR) are different. Precise size of vertical angle is important because it is used in conjunction with measured slope distance to compute horizontal and vertical distances. Small triangle formed by extending *S'* has hypotenuse equal to *X* and an angle of α - permits computation of side *X* cos α, which can be used together with *S* to determine $\alpha\Delta$. Therefore the elevation of monitoring target B is given by Equation (2.22) below:

$$Elev_B = Elev_A + hi + V - H \qquad \text{Eq.2.22}$$

Where,

$Elev_B$ = Elevation at point B

$Elev_A$ = Elevation at point A

hi = instrument height

V = vertical angle

HR = Height reflector

However, in this method, because sight distances cannot be balanced, it is important that the systematic effects of earth curvature and refraction, and inclination in the instrument's line of sight (collimation error), be removed [45]. Then the corrected

elevation difference, Δh, between two points is:

$$\Delta h = hi + S\cos v + h_{cr} - hr \qquad \text{Eq.2.23}$$

Where,

Δh	=	Elevation difference between two points
hi	=	instrument height
S	=	Slope distance
V	=	vertical angle
h_{cr}	=	Earth curvature
h_r	=	Rod reading

Where *hi* the instruments height above ground, S is is the slope distance between two points, *v* the vertical angle between the instrument and the target point, *z* the zenith angle, h_{CR} the Earth curvature and refraction correction given in Equation (2.24), and *hr* the rod reading. Earth curvature and refraction (*CR*) is 0.0675 when *D* is in units of meters or 0.0206 when *D* is units of feet.

$$h_{CR} = CR\left(\frac{D}{1000}\right)^2 \qquad \text{Eq.2.24}$$

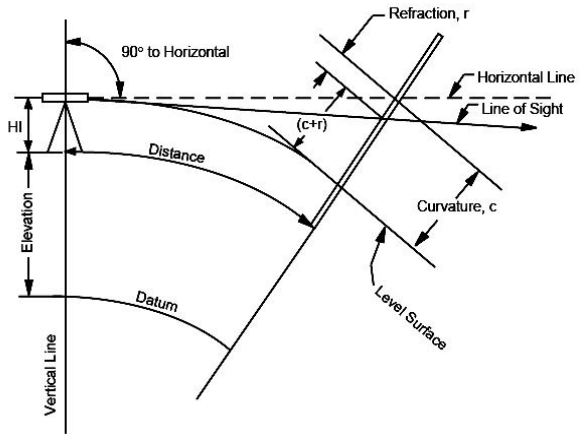

Figure 2.24 Curvatures and Refraction (CR)
(Source: B. Jackson and C. Leong)

Substituting the curvature and refraction formula into Equation 2.23 yields [46]

$$\Delta h = hi + S\cos v + CR\left(\frac{S\sin z}{1000}\right)^2 - hr \qquad \text{Eq.2.25}$$

Entering the partial derivatives and the standard errors of observation, the total error in trigonometric leveling is given below:

$$\sigma_{\Delta h} = \sqrt{\sigma_{hi}^2 + \sigma_{hr}^2 + \cos z + \frac{CR(S)\sin^2 z}{500{,}000}\sigma_s^2 + \frac{CR(S^2)\sin z\cos z}{500{,}000}\operatorname{Sen} z\frac{\sigma_z^2}{\rho}} \qquad \text{Eq.2.26}$$

Where *z* is the zenith angle, ρ is constant value of (206,264.8"/rad), *CR* is Earth curvature and refraction correction in meters, σ_{hi} is height of instrument error, σ_{hr} is target or prism error, $\sigma_z = \sqrt{2\sigma_{DIN}^2 + \sigma_D^2}$ is estimated error in zenith angle of total station and σ_s is the slope distance estimated errors as shown in Equation 2.27 below.

$$\sigma_S = \sqrt{\sigma_{hi}^2 + \sigma_{hr}^2 + \sigma_a^2 + \frac{\sigma_b}{1{,}000{,}000}S} \qquad \text{Eq.2.27}$$

2.11.4 Error Propagations in Traverse Survey

All angles (azimuths) and lengths should receive a small correction to force closure. Changing only one line's azimuth and length would probably involve corrections that would destroy some of that line's significance. Therefore the effects of errors in distance and azimuth observations will have an effect on the results of final coordinates which are computed from latitude and departure, as shown in Figure 2.25 or in others words distance or azimuth observation changes can cause changes in both latitude and departure, as shown in Figure 2.26.

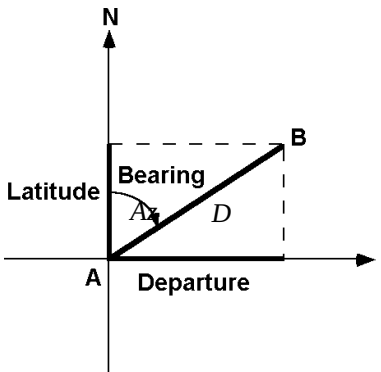

Figure 2.25 Latitude and Departure

From the above figure, the computation of the latitude and departure of a line is as presented in Equations 2.28a and 2.28b.

$$\text{Lat} = D \cos Az \qquad \text{Eq.2.28a}$$

$$\text{Dep} = D \sin Az \qquad \text{Eq.2.28b}$$

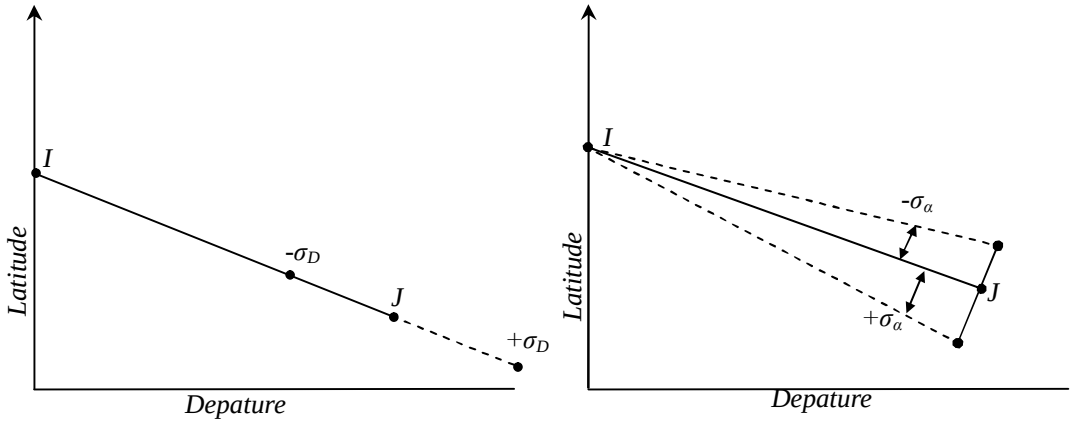

Figure 2.26 Latitude and Departure Errors on Distance (a) and azimuth (b)

Based on Figure 2.26 above, it is shown that distance and azimuth changes will affect latitude and departure. The estimated error in the line's latitude or departure can be derived from Equation 2.28 as expressed in Equation 2.29 below:

$$\frac{\partial Lat}{\partial D} = \cos Az \quad \frac{\partial Lat}{\partial Az} = -D \sin Az$$
$$\frac{\partial Dep}{\partial D} = \sin Az \quad \frac{\partial Dep}{\partial Az} = D \cos Az \qquad \text{Eq.2.29}$$

The estimated errors in these values are solved using matrix as described below:

$$\sum_{Lat,Dep} = \begin{bmatrix} \frac{\partial Lat}{\partial D} & \frac{\partial Lat}{\partial Az} \\ \frac{\partial Dep}{\partial D} & \frac{\partial Dep}{\partial Az} \end{bmatrix} \begin{bmatrix} \sigma_D^2 & 0 \\ 0 & \sigma_{Az}^2 \end{bmatrix} \begin{bmatrix} \frac{\partial Lat}{\partial D} & \frac{\partial Dep}{\partial D} \\ \frac{\partial Lat}{\partial Az} & \frac{\partial Dep}{\partial Az} \end{bmatrix} - \begin{bmatrix} \sigma_{Lat}^2 & \sigma_{Lat,Dep} \\ \sigma_{Lat,Dep} & \sigma_{Dep}^2 \end{bmatrix}$$

Substituting partial derivatives into the above yields:

$$\Sigma_{Lat,Dep} = \begin{bmatrix} \cos Az & -D\sin Az \\ \sin Az & D\cos Az \end{bmatrix} \begin{bmatrix} \sigma_D^2 & 0 \\ 0 & \sigma_{Az}^2 \end{bmatrix} \begin{bmatrix} \cos Az & \sin Az \\ -D\sin Az & D\cos Az \end{bmatrix} \qquad \text{Eq.2.30}$$

From Equation 2.30 above, the estimated errors of latitude and departure are obtainable by entering the distance and azimuth lines from the monitoring observations; whereby the estimated errors of distance and sum of azimuth can be computed from Equation 2.1 and 2.21 respectively. If the results show that the off-diagonal matrix $\sum_{Lat,Dep}$ is not equal to zero, its means that there are significant error in the line of observations, which has been explained earlier in Figure 2.26.

2.12 Data Screening

The processing of raw data is very important in deformation study because even though the deformation might be in millimeter. The adjustment of such survey networks requires all considerations with respect to elimination of errors and corrects estimation of measurement precisions. Any deformation survey must pay particular attention to errors in the survey so that gross or systematic errors do not affect the detection of movements.

Hence, repeated measurements are usually made, the measured mean values and the standard deviation (SD) of the observations are very important. All observation outliers such as gross errors must be eliminated. This is an observation that is much higher or lower than most of the other observations in the data set. Often, outliers represent some sort of error (i.e. measurement device malfunction, incorrect data recording, etc).

However, other outliers represent some sort of anomaly that may provide an insight into the process of data gathering. These values also have significant effect on the mean and standard deviation, and are therefore important to identify, as shown in Figure 2.27 above.

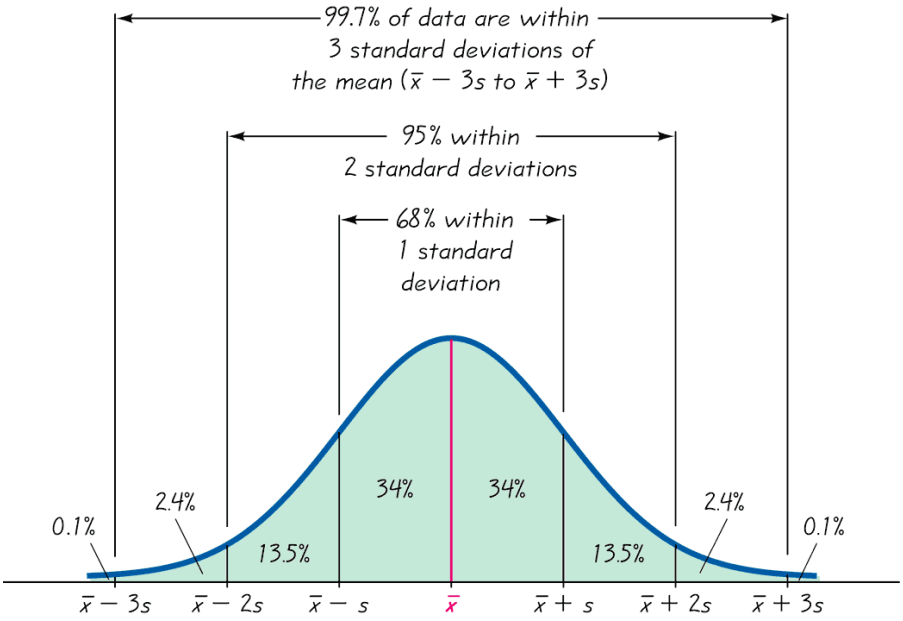

Figure 2.27 The "Rule of Thumb" of Three Standard Deviations (SD)

The "Rule of Thumb" of three standard deviations (SD) for measurement rejection corresponds to a confidence level of 99.7% for a normal distributed measurement. According to this rule of thumb, 25 times in 10000 measurements the expected gross error is ($\overline{x}$ – 3S) and ($\overline{x}$ + 3S), which are said to be the "critical value" or CVs [47] (Where $\overline{x}$ is mean of observation and S is a standard deviation). A critical value is used in significance testing. It is the value that a test statistic must exceed in order for the null hypothesis to be rejected.

2.13 Standard Deviation of Displacements

Point's displacements are calculated by differencing the adjusted coordinates for the

most recent survey campaign with the coordinates obtained at some reference time or by the difference in epoch observations. Each movement vector has a magnitude and direction which can be expressed as point displacement coordinate differences, as shown in Figure 2.28 and Equations 2.31 and 2.32 below. The displacement that exceeds the amount of movement expected under normal operating conditions will indicate possible abnormal behavior.

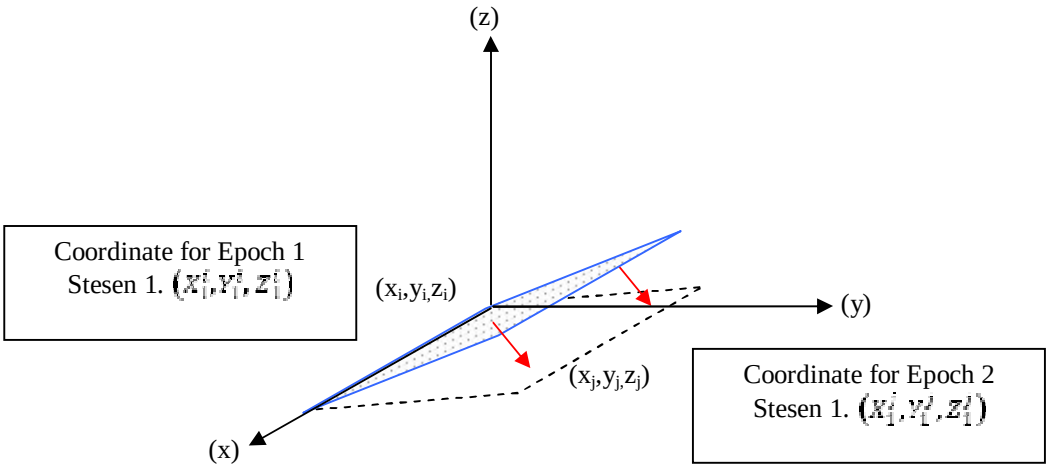

Figure 2.28 Calculation of Displacement

The magnitude of the horizontal displacement and direction of a station between i and j epoch (Δd_{ij}) are shown in the following Equations:

$$\Delta d_{ij} = \sqrt{\left[\left(X_1^j - X_1^i\right)^2 - \left(Y_1^j - Y_1^i\right)^2\right]} \qquad \text{Eq.2.31}$$

$$\alpha = \text{Tan}^{-1} = \left(\left[\frac{\left(X_1^j - X_1^i\right)}{\left(Y_1^j - Y_1^i\right)}\right]\right) \qquad \text{Eq.2.32}$$

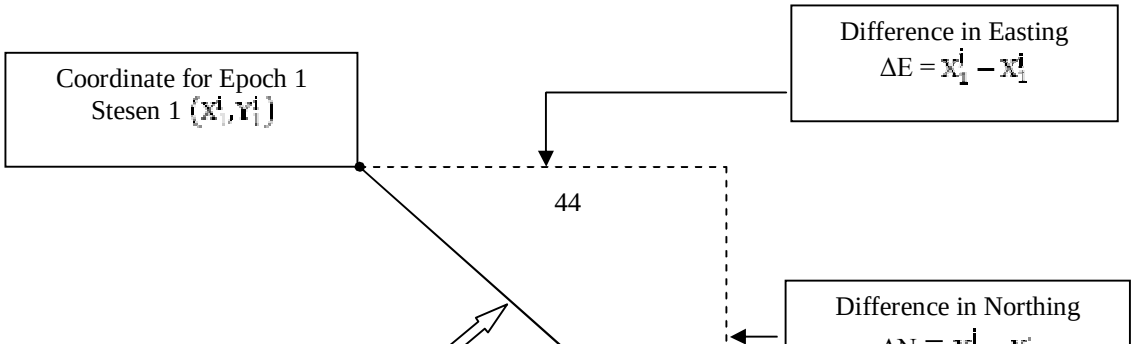

Figure 2.29 Calculation of Horizontal Displacement

The magnitude of the vertical displacement of a station between i and j epoch (Δv_{ij}) is shown in the following Equation:

$$\Delta v_{ij} = \left(Z_1^j - Z_1^i\right) \qquad \text{Eq.2.33}$$

Derivatives of the horizontal and vertical displacement Equations, as mentioned previously in Equations 2.31 and 2.33 is:

$$\sigma d^2 = \left(\frac{\delta d}{\delta x_j^2}\right)^2 (\sigma x_j^2)^2 + \left(\frac{\delta d}{\delta x_1^1}\right)^2 (\sigma x_1^1)^2 + \left(\frac{\delta d}{\delta y_j^2}\right)^2 (\sigma y_j^2)^2 + \left(\frac{\delta d}{\delta y_j^1}\right)^2 (\sigma y_1^1)^2$$

Eq.2.34

$$\sigma v^2 = \left(\frac{\delta v}{\delta z^1}\right)^2 (\sigma z^1)^2 + \left(\frac{\delta v}{\delta z^2}\right)^2 (\sigma z^2)^2 \qquad \text{Eq.2.35}$$

Substituting partial derivatives into the above yields:

$$\sigma d^2 = \left(\frac{x_1^2 - x_1^1}{d^{1/2}}\right)^2 (\sigma x_1^2)^2 + \left(\frac{x_1^2 - x_1^1}{d^{1/2}}\right)^2 (\sigma x_1^1)^2 + \left(\frac{y_1^2 - y_1^1}{d^{1/2}}\right)^2 (\sigma y_1^2)^2 + \left(\frac{y_1^2 - y_1^1}{d^{1/2}}\right)^2 (\sigma y_1^1)^2$$

Eq.2.36

$$\sigma v^2 = 1.(\sigma z^1)^2 + 1.(\sigma z^2)^2 \qquad \text{Eq.2.37}$$

2.14 Analysis of Displacement

The common method used in the analysis of displacements is by direct coordinate's differences between two epoch observations, since the final data are in coordinate form. However, in order to identify the unstable point, it is necessary to clean all the errors which can affect the results. Such errors could be propagations in distances, angles and elevation, if the monitoring survey works are carried out by using Total Station. The values of variances must be smaller than the magnitude of displacements [48].

At each step, a statistical assessment must be performed in order to test the significance of the estimated displacements. Finally, the interpretation of results at the interesting area of the monitoring structures or objects is attempted. After the adjustment of at least two epochs, it is possible to determine the displacement of a point d and displacement variance σd^2 is performed on the equations 2.31 and 2.36. In practice, a test for determination of statistical significance of displacement is often used [48], as the relation between the displacement and the displacement accuracy for horizontal and vertical components. The test statistic can be written as;

$$T = \frac{d_{horizontal}}{\sigma d} \qquad \text{Eq.2.38}$$

$$T = \frac{d_{vertical}}{\sigma v} \qquad \text{Eq.2.39}$$

It is important to note that the calculated displacement is not a linear function of variables Δy and Δx, therefore the test statistic from Equation 2.38 and 2.39 is not normally distributed. The probability function for the test statistic Equation 2.38 and 2.39 is determined empirically with simulations, and then compared to the critical value considering the chosen significance level α. The risk to reject the null hypothesis is too high. In such case, assume that the displacement is statistically non-significant. If the test statistic is higher than critical value, the risk to reject the null hypothesis is smaller than the chosen significance level α. Therefore, the hypothesis is justifiably rejected and can confirm the statistical significance of the displacement magnitude.

The null and alternative hypotheses are tested by the test statistic;

Null hypothesis $\quad Ho: \delta d_{ij} = 0, \quad$ Eq.2.40

Alternative hypothesis $\quad Ha: \delta d_{ij} \neq 0, \quad$ Eq.2.41

The test statistic for this test is: $\quad T = \frac{\delta d_{ij}}{\sigma(\delta d_{ij})} \quad$ Eq.2.42

which has a Student's t-distribution if *Ho* is true; the region where the null hypothesis is rejected is :

$$|T| = t_{df,\alpha/2} \quad \text{Eq.2.43}$$

Where *df* is the degree of freedom and α is the significance level used for the test.

These methods have been used by a many researchers to test the significance of displacements, such as monitoring of high rise building deformation using the GPS, deformation of volcano and landslide displacements in Indonesia using survey methods in order to check the significance of displacements [49]. Besides that, this approach also has been used in software development for deformation detection.

2.15 Summary of the Literature Review

From the literature review, it is obvious that landslide phenomenon is one of the dangerous and harmful natural disasters. The phenomenon can be more serious when the incident involved human casualties and expensive cost of properties damages. Currently, the location of potential landslide or slope failure can be anticipated, and identified but not the time of occurrences.

The deformation monitoring is focused on three main parts. The first part is to determine the suitable instruments that can be used for monitoring. However, each of the instruments and measurements technique has its own advantages and disadvantages. Therefore, in most cases the selection of most appropriate technique or combination of techniques for any particular application will depend on cost such as instruments technology, technical support or expertise, survey specification or procedures, the accuracies required, and the scale of the survey involved. Unfortunately, most of the methods cannot be applied in inaccessible and dangerous areas. Most of the existing methods involved large man power because of the need to install a co-operative device at the target; in tachometry a prism, in GPS a rover receiver. These means that somebody has to set up that device there and on the other hand, in satellite laser ranging the difficulty is to obtain approval from the authorized organization for accessing the satellite images. In addition, the latest technology such as laser scanning is still relatively expensive despite its high resolution. In consideration of human safety, accessibility to the measured location and hazardous environments, the reflector-less Total Station seems to offer a good solution. The instrument is highly effective when measuring to points located in dangerous areas or difficult to place prism directly, and when job efficiency is the first priority. The reflector-less Total Station is able to ensure safer work practices, reduce worker exposure to hazardous environments, and significantly reduce the survey crew size from three to one person.

The second part is the data processing; included in this part are the instrument calibration and error propagation in observations including systematic and random errors. Several preliminary researches and experiments on the application of reflector-less Total

Station have been conducted previously. Many manufacturers and vendors, ranging from optical to survey companies have introduced this technology, each claiming that their reflector-less TS has better accuracy. Therefore, a specific test must be performed in order to justify their statement. The approach from literature review of the calibration is very useful in this research. However, the testing must be carried out in a normal condition and with target materials that are suitable to the slope of the study area. The calibration result is very useful before the actual measurements and observation are carried out.

Angle and distance measurements are very important in this research where the accuracy of landslide prediction depend on the observations. Therefore the adjustment of the fundamental measurements is very important, due to propagation of errors. The general theory of random errors and systematic errors has been developed from the literature review. A simple method of adjustment can be used in order to isolate remaining blunders in the data captured by a reflector-less Total Station.

The third part is the assessment of movement and detection of deformation. This part is a very important component of this research, because the results are based on interpretation of the magnitude vector movement. There are many methods that have been adopted from previous researchers. Since this research is more focused on instrument application, the method of direct coordinate differences has been chosen for analyzing the results. Statistical tests were used to determine whether significant movements have occurred between the monitoring campaigns and the compared with the prism modes as a quality measured.